

Strangeness in Quark Matter, Levoča, Slovakia, June 2007

Rapidity-dependent chemical potentials in a statistical approach[‡]

Wojciech Broniowski

The H. Niewodniczański Institute of Nuclear Physics,
Polish Academy of Sciences, PL-31342 Kraków, Poland
Institute of Physics, Świętokrzyska Academy, PL-25406 Kielce, Poland

E-mail: Wojciech.Broniowski@ifj.edu.pl

Bartłomiej Biedroń

AGH University of Science and Technology, PL-30059 Kraków, Poland

E-mail: rockhouse@dione.ifj.edu.pl

Abstract. We present a single-freeze-out model with thermal and geometric parameters dependent on the position within the fireball and use it to describe the rapidity and transverse-momentum spectra of pions, kaons, protons, and antiprotons measured at RHIC at $\sqrt{s_{NN}} = 200$ GeV by BRAHMS. THERMINATOR is used to perform the necessary simulation, which includes all resonance decays. The result of the fit to the data is the expected growth of the baryon and strange chemical potentials with the spatial rapidity α_{\parallel} . The value of the baryon chemical potential at $\alpha_{\parallel} \sim 3$ is about 200 MeV, *i.e.* lies in the range of the highest SPS energies. The chosen geometry of the fireball has a decreasing transverse size as the magnitude of α_{\parallel} is increased, which also corresponds to decreasing transverse flow. The strange chemical potential obtained from the fit to the K^+/K^- ratio is such that the local strangeness density in the fireball is compatible with zero. The resulting rapidity spectra of net protons are described qualitatively within the statistical approach. As a result of our study, the knowledge of the “topography” of the fireball is acquired, allowing for other analyses and predictions.

PACS numbers: 25.75.-q, 25.75.Gz, 24.60.-k

Submitted to: *J. Phys. G: Nucl. Phys.*

[‡] Research supported by the Polish Ministry of Education and Science, grants N202 034 32/0918 and 2 P03B 02828.

More details of the presented material can be found in Ref. [1].

An important goal of relativistic heavy-ion physics is to find the “topography” of the system at freeze-out, *i.e.* to determine the dependence of thermal parameters on the location, in particular on the spatial rapidity $\alpha_{\parallel} = \frac{1}{2} \log(t-z)/(t+z)$. Numerous studies of the global particle ratios [2–18] can be divided into two categories: the 4π studies at low energies (SIS, AGS) and the analyses at mid-rapidity for approximately boost-invariant systems at high energies (RHIC). In the latter case the yields dN/dy vary only by a few percent in the window $|y| < 1$. When the system is not boost-invariant the task is more involved because particles detected at a given pseudorapidity may originate from different locations in the fireball. Thermal conditions and flow change from place to place, which should be taken into account. In addition, the resonance decays are more complicated to treat. As a result, a full-fledged simulation is necessary. We use THERMINATOR [19] with a suitably extended single-freeze-out model of Ref. [11, 12, 20]. We recall the approach reproduces in an efficient way the transverse-momentum spectra, including strange particles [20], the production of resonances [21], the charge balance functions [22], the elliptic flow [23], the HBT radii [24], and the transverse energy [25, 26]. To fix the model parameters we use the data from the BRAHMS collaboration at $\sqrt{s_{NN}} = 200$ GeV [27–30].

Our extension to boost-non-invariant systems consists of two elements: the choice of the freeze-out hypersurface and the collective flow, as well as incorporation of the dependence of thermal parameters on the location. We use the freeze-out hypersurface parameterized as

$$x^{\mu} = \tau (\cosh\alpha_{\perp} \cosh\alpha_{\parallel}, \sinh\alpha_{\perp} \cos\phi, \sinh\alpha_{\perp} \sin\phi, \cosh\alpha_{\perp} \sinh\alpha_{\parallel}). \quad (1)$$

The parameter τ is the proper time at freeze-out, and α_{\perp} is related to the transverse radius, $\rho = \sqrt{x^2 + y^2} = \tau \sinh\alpha_{\perp}$. The four-velocity is chosen to follow the Hubble flow $u^{\mu} = x^{\mu}/\tau$. In the boost-invariant model ρ was limited by the space-independent parameter ρ_{\max} , or $0 \leq \alpha_{\perp} \leq \alpha_{\perp}^{\max}$. Now we take

$$0 \leq \alpha_{\perp} \leq \alpha_{\perp}^{\max}(\alpha_{\parallel}) \equiv \alpha_{\perp}^{\max}(0) \exp\left(-\frac{\alpha_{\parallel}^2}{2\Delta^2}\right). \quad (2)$$

The interpretation of Eq. (2) is following: as we depart from the center, increasing $|\alpha_{\parallel}|$, we simultaneously reduce α_{\perp} , or ρ_{\max} . The rate of this reduction is controlled by a new model parameter, Δ . In other words, the fireball gets thinner and thinner as we depart from the central rapidity region. The geometry and expansion of the fireball are described by three parameters: τ , controlling the overall abundance of particles, $\rho_{\max}^{(0)}$, influencing the slope of the p_T -spectra, and Δ , controlling the fall-off of the rapidity spectra. With the standard parameterization of the particle four-momentum in terms of rapidity and the transverse mass, $p^{\mu} = (m_{\perp} \cosh y, p_{\perp} \cos\varphi, p_{\perp} \sin\varphi, m_{\perp} \sinh y)$, we find

$$\begin{aligned} p \cdot u &= m_{\perp} \cosh(\alpha_{\perp}) \cosh(\alpha_{\parallel} - y) - p_{\perp} \sinh(\alpha_{\perp}) \cos(\phi - \varphi), \\ d^3\Sigma \cdot p &= \tau^3 d\alpha_{\parallel} d\phi \sinh\alpha_{\perp} d\alpha_{\perp} p \cdot u \end{aligned} \quad (3)$$

where $d^3\Sigma^{\mu}$ is the volume element of the hypersurface. These expressions are used the Cooper-Frye [31] formula for the momentum density of a given species of *primordial* particles:

$$\frac{d^2N}{2\pi p_T dp_T dy} = \tau^3 \int_{-\infty}^{\infty} d\alpha_{\parallel} \int_0^{\alpha_{\perp}^{\max}(\alpha_{\parallel})} d\alpha_{\perp} \int_0^{2\pi} d\phi p \cdot u f(\beta p \cdot u - \beta\mu(\alpha_{\parallel})), \quad (4)$$

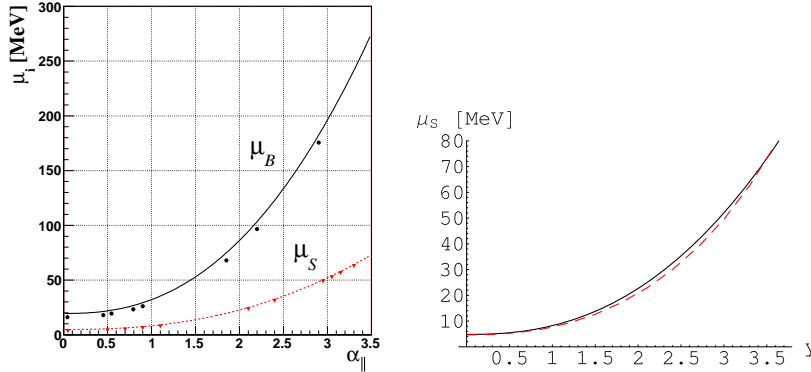


Figure 1. Left: the model baryon and strange chemical potentials plotted as functions of α_{\parallel} . Parameters of Eq. (5) are obtained from the fit to the BRAHMS data [27, 28]. The points represent a naive calculation based of Eq. (6). Right: Comparison of μ_S obtained from the fit to the data (solid line) and from μ_B and the condition of zero local strangeness density (dashed line).

where $p \cdot u$ is taken at $\varphi = 0$ (azimuthal symmetry), f denotes the Bose-Einstein or Fermi-Dirac statistical distribution function, $\beta = 1/T$, and $\mu(\alpha_{\parallel}) = B\mu_B(\alpha_{\parallel}) + S\mu_S(\alpha_{\parallel}) + I_3\mu_{I_3}(\alpha_{\parallel})$, with B , S , and I_3 denoting the baryon number, strangeness, and the third component of isospin of the given particle. Thus we admit the dependence of chemical potentials on α_{\parallel} . In general, the temperature T also depends on α_{\parallel} . In this work, however, we apply the model for not too large values of rapidity, $|y| \leq 3.3$, where the obtained values for μ_B are less than ~ 250 MeV. The universal freeze-out curve [8] gives a practically constant value of T in this range, thus we fix $T = 165$ MeV everywhere.

The functional form of the chemical potentials is parameterized as follows:

$$\mu_i(\alpha_{\parallel}) = \mu_i(0) \left[1 + A_i \alpha_{\parallel}^2 \right], \quad i = B, S, I_3. \quad (5)$$

Practice shows that to a good approximation the statistical distributions may be replaced by the Boltzmann factors. Then the integrand of Eq. (4) contains the term $\exp[-\beta m_{\perp} \cosh(\alpha_{\perp}) \sinh(\alpha_{\parallel} - y) + \beta \mu(\alpha_{\parallel})]$. The relevant integration range in α_{\parallel} is sharply peaked around $\alpha_{\parallel} \simeq y$, thus the chemical potentials are taken approximately at $\mu_i(\alpha_{\parallel}) \simeq \mu_i(y)$ and the factors $\exp[\beta \mu(y)]$ can be pulled out from the integration. As a result, the following *approximate* relations for the ratios of yields hold:

$$\frac{p}{\bar{p}} \simeq \exp(2\beta\mu_B), \quad \frac{K^+}{K^-} \simeq \exp(2\beta\mu_S), \quad \frac{\pi^+}{\pi^-} \simeq \exp(2\beta\mu_{I_3}). \quad (6)$$

Upon inversion $\mu_B(y) \simeq \frac{1}{2}T \log(p/\bar{p})$, *etc.* With the help of these approximate equalities we set the starting values of the parameters $\mu_i(0)$ and A_i , which are then iterated by THERMINATOR to fit the data. The Δ parameter is fixed with the pion rapidity spectra $dN_{\pi^{\pm}}/dy$, with the optimum value of $\Delta = 3.33$. The other geometric parameters are taken from earlier fits to mid-rapidity p_T -spectra: $\tau = 9.74$ fm, $\rho_{\max}(z=0) = 7.74$ fm.

The result of our optimization is shown in Fig. 1. The optimum parameters are:

$$\begin{aligned} \mu_B(0) &= 19 \text{ MeV}, \quad \mu_S(0) = 4.8 \text{ MeV}, \quad \mu_{I_3}(0) = -1 \text{ MeV}, \\ A_B &= 0.65, \quad A_S = 0.70, \quad A_{I_3} = 0. \end{aligned} \quad (7)$$

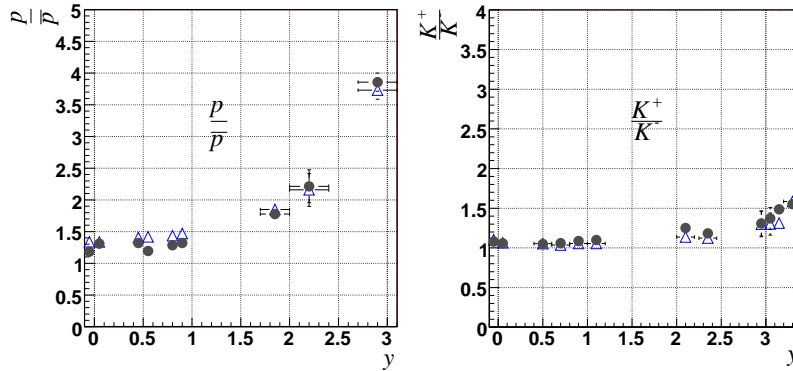


Figure 2. Dependence of particle ratios on rapidity: left – p/\bar{p} , right – K^+/K^- . The open triangles are the Brahms data [27, 28], while the filled circles show the result of the model simulation. The data for p and \bar{p} are not corrected for the feed-down from weak-decays [27].

We observe the expected behavior for the baryon chemical potential, which increases with $|\alpha_{\parallel}|$. The value at the origin is 19 MeV, somewhat lower than the earlier mid-rapidity fits made in boost-invariant models in Refs. [11, 32], yielding 26 MeV. The lower value in our case is well understood. The previous mid-rapidity fits include the data in the range $|y| \leq 1$. This range collects the particles emitted from the fireball at $|\alpha_{\parallel}| \leq 2$, hence the value of μ_B in the previous mid-rapidity fits is an average of our $\mu_B(\alpha_{\parallel})$ over the range, approximately, $|\alpha_{\parallel}| \leq 2$, with some weight proportional to the particle abundance. A similar effect occurs for μ_S . We do not incorporate corrections for the feed-down from weak decays (*i.e.* all the decays are included), since this is the policy of Ref. [27] for the treatment of p and \bar{p} .

We note that at $\alpha_{\parallel} = 3$ the value of μ_B is 200 MeV. This value is comparable to the highest-energy SPS fit ($\sqrt{s_{NN}} = 17$ GeV), where $\mu_B \simeq 230$ MeV. The behavior of the strange chemical potential is qualitatively similar. It also increases with $|\alpha_{\parallel}|$, growing from 5 MeV at the origin to 50 MeV at $\alpha_{\parallel} = 3$. The ratio $\mu_B(\alpha_{\parallel})/\mu_S(\alpha_{\parallel})$ is very close to a constant $\simeq 4 - 3.5$. The dots in the left panel of Fig. 1 show the result of the naive calculation of Eq. (6). We note that these points are close to the result of the full-fledged fit of our model. This is of practical use, since the application of Eq. (6) involves no effort (as done *e.g.* in Ref. [33–35]), while the full model simulation incorporating resonance decays, flow, *etc.*, is costly.

There is another interesting point. In thermal models one may obtain the local value of the strange chemical potential, μ_S , at a given μ_B with the condition of the vanishing strangeness density, $\rho_S = 0$. The result is shown in Fig. 1, where we compare the strange chemical potential obtained from the fit to the data (solid line) and from the condition of zero local strangeness density at a given $\mu_B(\alpha_{\parallel})$ (dashed line). The two curves turn out to be virtually the same. This shows that the net strangeness density in our fireball is, within uncertainties of parameters, *compatible with 0*. This is not obvious from the outset, as the condition of zero strangeness density is not assumed in our fitting procedure. Although this feature is natural in particle production mechanisms, in principle only the total strangeness, integrated over the whole fireball, must be initially zero. Variation of the strangeness density with α_{\parallel} is admissible, but turns out not to occur.

Figure 2 shows the quality of our fit of the parameters of the chemical potentials, Eq.(7), for the ratios p/\bar{p} and K^+/K^- . In Fig. 3 we compare the obtained rapidity

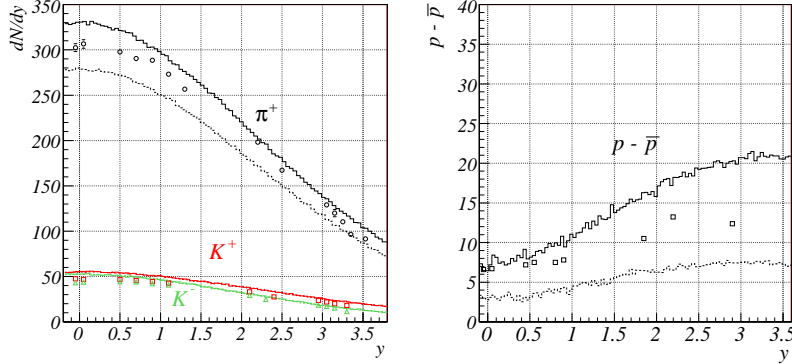


Figure 3. Left: Rapidity spectra of π^+ , K^+ , and K^- . The data come from Refs. [27, 28] (circles – π^+ , squares – K^+ , triangles – K^-), while the histogram lines show the model results. For π^+ the solid (dashed) line corresponds to the full feeding (no feeding) from the weak hyperon decays. The experimental pion yields are corrected for weak decays [28]. Right: spectrum of net protons, $p - \bar{p}$. The data points come from Refs. [27, 28], while the solid (dashed) histogram lines show the result of the model simulation with full feeding (no feeding) from the weak hyperon decays. Data points should be compared to the model with full feeding (solid lines).

spectra of π^+ , K^+ , and K^- to the experiment. The experimental yields for the pions are corrected for the feed-down from the weak decays as described in Ref. [28]. For that reason for the case of π^+ we give the model predictions with the full feeding from the weak decays (solid line) and with no feeding at all (dashed line). We note a reasonable agreement, with the data falling between the two extreme cases. The spectra of kaons are also reproduced reasonably well. We see from the right panel of Fig. 3 that the qualitative growing of the net-proton spectrum with y is reproduced. Note that predictive power is left for this observable, as only the ratio \bar{p}/p is used to fit μ_B . The model curves with and without the weak-decays correction embrace the experimental points.

Here are the highlights this talk:

- (i) Decreasing yields of particles with rapidity require that the system becomes colder, thinner, or more dilute as one departs from mid-rapidity. In our analysis for the highest RHIC energies we take it to be thinner, keeping the temperature constant.
- (ii) The naive extraction of the baryon and strange chemical potentials from ratios of p/\bar{p} and K^+/K^- according to Eq. (6) works surprisingly well, as shown in the comparison to the full calculation in Fig. 1. This is because at $\sqrt{s_{NN}} = 200$ GeV the dependence of yields on α_{\parallel} does not depart much from linearity within one unit of rapidity, which is the window contributing to the α_{\parallel} integration in Eq. (4). In addition, the feeding contributions from resonance decays to both particles in the ratio are approximately proportional to each other. At lower energies (SPS) the naive extraction should not work.
- (iii) The baryon and strange chemical potentials grow with α_{\parallel} , reaching at $y \sim 3$ values close to those of the highest SPS energies of $\sqrt{s_{NN}} = 17$ GeV. This agrees with the conclusions of Roehrich [36].
- (iv) At mid-rapidity the values of the chemical potentials are even lower than derived

from the previous thermal fits to the data for $|y| \leq 1$, with our values taking $\mu_B(0) = 19$ MeV and $\mu_S(0) = 5$ MeV. The reason for this effect is that the particle with $|y| \leq 1$ originate from a region $|\alpha_{\parallel}| \leq 2$, and on the average the effective values of chemical potentials are larger compared to the values at the very origin (cf. Fig. 1).

- (v) The local strangeness density of the fireball is compatible with zero at all values of α_{\parallel} . Although this feature is natural in particle production mechanisms, here it has been obtained independently just from fitting the chemical potentials to the data.
- (vi) The ratio of the baryon to strange chemical potentials varies very weakly with rapidity, ranging from ~ 4 at midrapidity to ~ 3.5 at larger rapidities.
- (vii) The $d^2N/(2\pi p_{\perp} dp_{\perp} dy)$ spectra of pions and kaons are also well reproduced [1], complying to our hypothesis for the shape of the fireball in the longitudinal direction.
- (viii) The feature of the increasing yield of the net protons, $p - \bar{p}$, with rapidity is obtained naturally, explaining qualitatively the shape of the rapidity dependence on purely statistical grounds.

- [1] B. Biedroń, W. Broniowski, Phys. Rev. C75 (2007) 054905.
- [2] P. Koch, J. Rafelski, South Afr. J. Phys. 9 (1986) 8.
- [3] J. Cleymans, H. Satz, Z. Phys. C57 (1993) 135.
- [4] J. Sollfrank, M. Gazdzicki, U. W. Heinz, J. Rafelski, Z. Phys. C61 (1994) 659.
- [5] P. Braun-Munzinger, J. Stachel, J. P. Wessels, N. Xu, Phys. Lett. B344 (1995) 43.
- [6] M. Gazdzicki, M. I. Gorenstein, Acta Phys. Polon. B30 (1999) 2705.
- [7] G. D. Yen, M. I. Gorenstein, Phys. Rev. C59 (1999) 2788.
- [8] J. Cleymans, K. Redlich, Phys. Rev. Lett. 81 (1998) 5284.
- [9] F. Becattini, J. Cleymans, A. Keranen, E. Suhonen, K. Redlich, Phys. Rev. C64 (2001) 024901.
- [10] J. Rafelski, J. Letessier, Phys. Rev. Lett. 85 (2000) 4695–4698.
- [11] W. Broniowski, W. Florkowski, Phys. Rev. Lett. 87 (2001) 272302.
- [12] W. Broniowski, A. Baran, W. Florkowski, Acta Phys. Polon. B33 (2002) 4235–4258.
- [13] F. Becattini, M. Gazdzicki, A. Keranen, J. Manninen, R. Stock, Phys. Rev. C69 (2004) 024905.
- [14] P. Braun-Munzinger, K. Redlich, J. Stachel, in Quark Gluon Plasma 3, ed. R. C. Hwa and X. N. Wang (World Scientific, Singapore, 2004).
- [15] G. Torrieri, J. Rafelski, J. Phys. G30 (2004) S557.
- [16] J. Cleymans, B. Kampfer, M. Kaneta, S. Wheaton, N. Xu, Phys. Rev. C71 (2005) 054901.
- [17] J. Rafelski, J. Letessier, G. Torrieri, Phys. Rev. C72 (2005) 024905.
- [18] F. Becattini, L. Ferroni, J. Phys. G31 (2005) S1091.
- [19] A. Kisiel, T. Taluc, W. Broniowski, W. Florkowski, Comput. Phys. Commun. 174 (2006) 669.
- [20] W. Broniowski, W. Florkowski, Phys. Rev. C65 (2002) 064905.
- [21] W. Broniowski, W. Florkowski, B. Hiller, Phys. Rev. C68 (2003) 034911.
- [22] P. Bożek, W. Broniowski, W. Florkowski, Acta Phys. Hung. A22 (2005) 149.
- [23] W. Broniowski, A. Baran, W. Florkowski, AIP Conf. Proc. 660 (2003) 185.
- [24] A. Kisiel, W. Florkowski, W. Broniowski, Phys. Rev. C73 (2006) 064902.
- [25] D. Prorok, Eur. Phys. J. A26 (2005) 277.
- [26] D. Prorok, Phys. Rev. C73 (2006) 064901.
- [27] I. G. Bearden, et al., Phys. Rev. Lett. 90 (2003) 102301.
- [28] I. G. Bearden, et al., Phys. Rev. Lett. 94 (2005) 162301.
- [29] M. Murray, these proceedings.
- [30] P. Staszal, these proceedings.
- [31] F. Cooper, G. Frye, Phys. Rev. D10 (1974) 186.
- [32] P. Braun-Munzinger, D. Magestro, K. Redlich, J. Stachel, Phys. Lett. B518 (2001) 41.
- [33] J. Cleymans, these proceedings.
- [34] J. Cleymans, these proceedings.
- [35] F. Becattini, J. Cleymans, J. Phys. G34 (2007) S959.
- [36] D. Roehrich, talk at Critical Point and Onset of Deconfinement (Florence, 36 July, 2006).